

# Characterization of Surface and Trapped Dust Samples Collected around Human Settlements That are in the Vicinity of Old Mine Tailings in Mpumalanga Province, South Africa

Shadung J Moja<sup>1,2\*</sup>, Maphuti G Kwata<sup>1,2</sup>, Lerato M Sebesho<sup>3</sup>, Khuthadzo G Masindi<sup>1</sup> and Fanyana Mtunzi<sup>4</sup>

<sup>1</sup>Sustainable Resources and Environment Competency, Council of Geoscience, 280 Pretoria Street, Silverton, Pretoria, 0001, South Africa.

<sup>2</sup>Department of Environmental Sciences, Florida Campus, University of South Africa, P O Box X6, Florida, 1710, South Africa

<sup>3</sup>Engineering Competency, Council of Geoscience, 280 Pretoria Street, Silverton, Pretoria, 0001, South Africa.

<sup>4</sup>Department of Chemistry, Faculty of Applied and Computer Sciences, Vaal University of Technology, Private Bag X021, Vanderbijlpark, 1900, South Africa.

## Abstract

Asbestos mining is banned in many countries because of the health effects that are linked to the inhalation of asbestos dust/fibres. Most of asbestos mine tailings in Mpumalanga Province are not rehabilitated and dust/fibres are easily eroded by weather and settle in sensitive areas like human settlements. Surface and trapped dust samples were collected around human settlements that are in the vicinity of five abandoned and ownerless asbestos mine tailings in October 2015. After collection, surface dust samples were sieved with a 100 µm pore size stainless steel sieve to remove large dust particles. Trapped dust material was collected outdoors around the window panes in houses, on surfaces of old furniture and on windscreens of old cars. Surface and trapped dust samples were treated in the laboratory in preparation of analyses by the Scanning Electron Microscope – Energy Dispersive Spectrometry (SEM - EDS), X-Ray Diffraction (XRD) and X-Ray Fluorescence (XRF) techniques. Both the serpentine ( $Mg_3Si_2O_5(OH)_4$ ) and amphibole [ $Ca_2(Fe, Mg)_5Si_8O_{22}(OH)_2$ ] asbestos mineral groups were detected from the samples. Other silicate minerals present include the quartz ( $SiO_2$ ), talc [ $Mg_3Si_3O_{10}(OH)_3$ ], feldspar [(KAlSi<sub>3</sub>O<sub>8</sub>)-(NaAlSi<sub>3</sub>O<sub>8</sub>)-(CaAl<sub>2</sub>Si<sub>2</sub>O<sub>8</sub>)] and smectite [(Na,Ca)0.33(Al, Mg)<sub>2</sub>(Si<sub>4</sub>O<sub>10</sub>)(OH)<sub>2</sub>·nH<sub>2</sub>O]. Non silicates minerals which were detected are hematite (Fe<sub>2</sub>O<sub>3</sub>), chlorite (ClO<sup>2-</sup>), magnetite (Fe<sub>3</sub>O<sub>4</sub>), gibbsite [Al(OH)<sub>3</sub>], dolomite [Ca-Mg (CO<sub>3</sub>)<sub>2</sub>] and ilmenite (FeTiO<sub>3</sub>). Industrial and biological materials that include fly ash particles, organic and glass fibres were also detected. While the amounts detected are at trace levels, but the continued presence of asbestos minerals around residential areas is of concern.

**Keywords:** Dust particles; Asbestos fibers; Physico-chemical; Characterization; SEM-EDS; XRD; XRF; Mpumalanga; South Africa

## Introduction

The South African mining industry is highly developed due to the exploitation of vast natural mineral deposits and large reserves such as gold, platinum, coal and diamond [1,2]. While the mining industry has contributed significantly to the development of local economy and infrastructure, it has also degraded the natural environment [3]. Mining operations, owned and ownerless, contribute to seepage of contaminated water, dust pollution problems, contamination of soil, surface and ground water [4-6].

Most importantly, a large number of old mining operations have been abandoned and are now ownerless [7]. Some of these mine operations and the resultant mine tailing dumps have not been remediated or rehabilitated and are now characterized by illegal mining activities [5,8,9]. Although it's an illegal activity, illegal mining is increasing in the country due to poverty, unemployment, large number of illegal immigrants, organized crime syndicates etc. [10].

The most common asbestiform minerals that were mined and milled in South Africa are the chrysotile (also known as white asbestos), which is part of serpentine group, and the amosite (brown asbestos) and crocidolite (blue asbestos) that are part of the amphibole [3,11]. Historically, crocidolite and amosite amphibole asbestos group were mined in the Cape Northern Cape and Limpopo Province asbestos fields [8,12]. The asbestos mineral deposit in the Pietersburg asbestos field were many, small, scattered and were considered to be of lower grade than the crocidolite deposits in the Northern Cape Province. The amosite asbestos field were predominantly found in Mpumalanga and Limpopo Provinces [11]. The chrysotile – serpentine asbestiform is located mainly around the Barberton area (Kaapsehoop and Msauli)

within the ultramafic complexes intrusions associated with the ancient greenstones belts on the Kaapvaal Craton [8,13,14].

Asbestos minerals have been mined locally mainly for export purposes because of its wide application in commercial applications [3,15]. Local market of asbestos building material includes its usage in asbestos roof cement sheets and vinyl floor tiles [3,11,16]. Around the 1970's, South Africa was the third largest producer of asbestos after Canada and Russia [2]. On the global scale, the country produced all amosite and over 95% of crocidolite minerals [3]. But, the link between the exposure to asbestos dust with serious health effects led to the reduction of the overseas markets and sales dropped [17]. The regulations that banned the use, manufacture, import and export of asbestos and asbestos containing products in South Africa began in 2001 and was promulgated by the Department of Environmental Affairs and Tourism (DEAT) in 2008, but the actual mining or milling operations were closed in 2002 [3,18].

The tailings dumps contribute to the unsightly landscape and the

**\*Corresponding author:** Shadung John Moja, Sustainable Resources and Environment Competency, Council of Geoscience, 280 Pretoria Street, Silverton, Pretoria, 0001, South Africa, Tel no: +27 12 841 1485; Fax no: +27 86 513 2274; E-mail: [sjmoja@geoscience.org.za](mailto:sjmoja@geoscience.org.za)

**Received** May 23, 2016; **Accepted** June 27, 2016; **Published** July 03, 2016

**Citation:** Moja SJ, Kwata MG, Sebesho LM, Masindi KG, Mtunzi F (2016) Characterization of Surface and Trapped Dust Samples Collected around Human Settlements That are in the Vicinity of Old Mine Tailings in Mpumalanga Province, South Africa. J Earth Sci Clim Change 7: 360. doi: [10.4172/2157-7617.1000360](https://doi.org/10.4172/2157-7617.1000360)

**Copyright:** © 2016 Moja SJ, et al. This is an open-access article distributed under the terms of the Creative Commons Attribution License, which permits unrestricted use, distribution, and reproduction in any medium, provided the original author and source are credited.

characteristic fine asbestos material which makes it more susceptible to natural weathering processes [11]. The continued existence of un-rehabilitated asbestos mine tailings dumps and decommissioned old mine operations continue to pose human health and safety problems to nearby human settlements. Safety concerns from open shafts continue to be a problem [7]. Asbestos particles are microscopic in size and could be lifted from the asbestos rich rock or surface soil into the air by wind erosion and during excavating processes [15].

Individuals who inhale contaminated ambient air in occupational settings or residential areas that are closer to the asbestos mine sources are more at risk [16]. Some of the health effects associated with the breathing of asbestos fine dust include the non-cancer respiratory effects (such as asbestosis), mesothelioma (a rare type of cancer of the membrane around the lungs and body cavities) and lung cancer [3,8].

In this study, surface and trapped dust samples from human settlements that are nearby asbestos mine tailings were characterized to establish their mineral composition and levels.

## Materials and Methods

### Study area and location of sampling sites

This study took place within residential areas in Mpumalanga Province that are in the vicinity of asbestos mine tailings situated closer to residential areas around Nelspruit, Malelane and Msauli towns. Nelspruit is the provincial capital and is centrally situated, Malelane is on the eastern direction of Nelspruit and Msauli is located closer to the Swaziland border in the southern direction.

The Drakensburg mountain range with heights of more than 2000 m contributes to the amazing local landscape [19]. The most dominant vegetation found in the province includes the alpine grassland and the afro-montane forest which are common in areas that are well watered [19,20].

The geology within the study areas consist of the Barberton Greenstone Belt (BGB) located in north-eastern South Africa and forms part of the Archean Kaapvaal Craton [21,22]. The lowermost, ca. 8–10 km thick, 3.57–3.30 Ga-old Onverwacht Group is mainly composed of mafic to ultramafic volcanics, such as komatiites and basalts; cherts are subordinate [15,23]. The Nelspruit area consists of a cluster of giant rocks, quartzites of the Black Reef formation of the Transvaal Super Group [13]. The ultramafic or peridotite rock is made primarily of the olivine and pyroxene minerals and minor aggregates of mafic minerals such as plagioclase feldspar and amphibole [23].

Figure 1 shows the asbestos mine fields and sampling sites symbolized by the red triangular and multi-coloured circular icons, respectively. Sites A, B and C are centrally located outside Nelspruit, site D is located close to Malelane on the east and Site E is closer to Masauli in the south of the province. Surface and trapped dust samples were collected around five (5) human settlements and the sampling sites were within 5 km of the nearest abandoned and ownerless mine tailings. The highest estimated mine tailings height was about 45 m.

### Sample collection, treatment and analyses

About 2 kg of representative surface bulk dust samples were

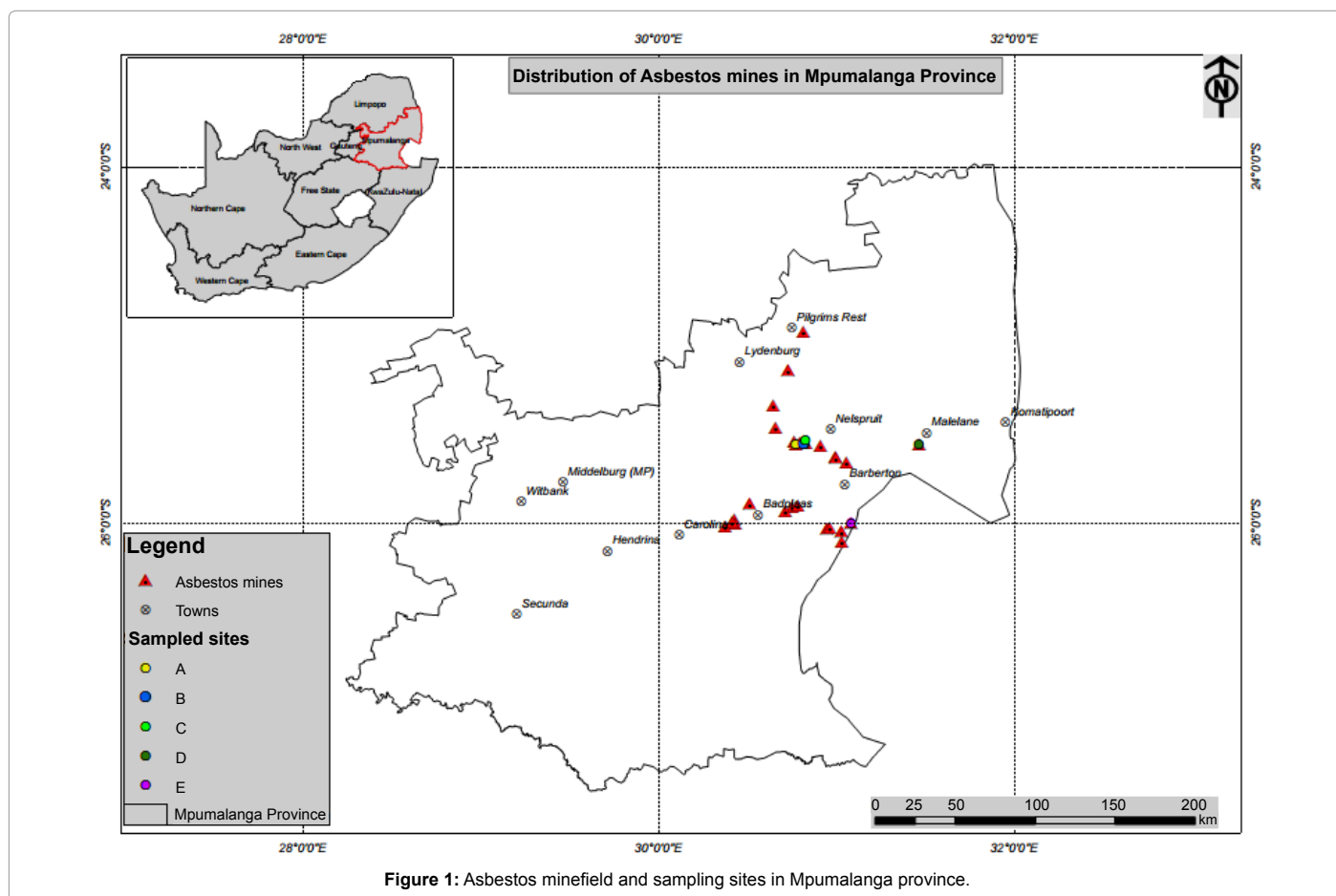


Figure 1: Asbestos minefield and sampling sites in Mpumalanga province.



Figure 2: Photos showing how and where surface dust samples were collected.



Figure 3: Photos showing how and where trapped dust samples were collected.

collected from different points at each sampling site by gently sweeping surface of earth with a clean nylon broom into a thoroughly washed plastic scoop (See Figure 2). The sampler faced in direction of the prevailing wind to minimized exposure to airborne dust particles. The scoop was thoroughly washed with dilute acid and thereafter rinsed with deionised water and dried between sample collections in order to avoid cross contamination. The collected dust samples were thereafter placed into well labeled, self-sealing propylene bags, stored in black plastic bags and transported to the laboratory. In the laboratory, the collected dust samples were air dried on a propylene sheet overnight. The air-dried dust samples were sieved with a 100  $\mu\text{m}$  stainless steel sieve to remove large materials.

Fine dust samples that collect on hard surfaces such as the top of kitchen units, windscreens of parked cars were collected by sticking them on sellotape (Figure 3). Samples were stored and preserved in labelled plastic storage container until they were analysed in the analytical laboratory. Since the sampling sites were far from each other, sampling took more than two weeks in October 2015.

### Instrumentation and measurement conditions

The XRD, SEM-EDS and XRF analytical instruments were conditioned according to the CGS Mineralogy Laboratory Methods [24].

X-Ray Diffraction data was obtained on BRUKER D8 Advance diffractometer with Cu radiation. The system is equipped with a LynxEye detector and a Ni-filter. Tape samples were mounted on dedicated filter holders or powder mounts and run in step scan mode from 2 to 70° 2 $\theta$  CuK ( $\lambda=1.54060$ ) radiation at a speed of 0.05° 2 $\theta$  steps size/1 sec and generator settings of 40 kV and 40 mA. Data processing, evaluation and reporting: XRD: Phase identification is based on BRUKER DIFFRAC Plus - EVA evaluation program. Phase concentrations are determined as semi quantitative estimates (with accuracy  $\pm 5\%$ ) using RIR (Reference Intensity Ratio) method and relative peak heights/areas proportions.

SEM/EDS analysis was performed on a Leica Stereoscan 440 SEM linked to an OXFORD INCA EDS. The system is equipped with an Oxford X-Max SDD detector with 20 mm<sup>2</sup> active area and resolution of about 128eV for Mn K $_{\alpha}$  (5895 eV) and has the capabilities for secondary, backscattered and cathode-luminescence electron imaging, X-Ray EDS microanalysis and X-Ray element mapping. Mineral chemistry was determined by means of spot analyses at beam settings of 20kV accelerating voltage, probe current of 5.0 nA and counting time was set at 100 s.

Sample preparation and processing: The dust trapped on cello tape samples are mounted on specialized filter holders and used for both XRD and SEM investigations. Where possible, dust was extracted from the filters and analyzed by XRD as powder specimens. For SEM study, powders are prepared as grain mounts. All specimens for SEM are coated with carbon to provide a conductive surface for optimum imaging and X-ray microanalysis.

SEM/EDS analysis was done at ~800-1000 times magnification depending on particle size and distribution with the brightness/contrast settings adjusted to highlight the minerals of interest. The results are presented in form of backscattered electron (BE) images for each sample.

For major element analysis, previously sieved surface dust samples were milled to produce size fraction of <75  $\mu\text{m}$ , which was roasted at 1000°C for at least 3 hours to oxidise Fe<sup>2+</sup> and S and to determine the loss of ignition (L.O.I.) in a muffle furnace. Glass disks were prepared by fusing about 1g of roasted sample and about 10 g flux consisting of 49.5% Li<sub>2</sub>B<sub>4</sub>O<sub>7</sub>, 49.5% LiBO<sub>2</sub> and 0.50% LiI at 1150°C. Quality control/quality assurance was done by using an in-house amphibolite reference material (sample 12/76). Also, 1 in every 10 samples was duplicated during sample preparation. For trace element analysis, about 12 g of milled sample and about 3 g Lico wax were mixed and pressed into a powder briquette by a hydraulic press with the applied pressure at 25 ton. The glass disks and wax pellets was analysed by a PAN analytical

wavelength dispersive Axios X-ray fluorescence spectrometer equipped with a 4 kW Rh tube.

## Results and Discussion

### Observation during fieldwork

Observation during the field work shows that all asbestos mine tailings were not rehabilitated and are visible from the nearby communities. Mine tailing closer to sampling sites A and C are bare, while others are partially covered by natural growing vegetation (Figure 4). Fine asbestos dust from these sites could easily be blown away by wind or be eroded by rain from these sources to nearby vulnerable areas.

### Quality assurance and control processes

The performance of the XRF against the Certified Soil Sample 12/79 shows acceptable % recoveries of the metal oxides that ranged

from 98.65 for  $\text{Cr}_2\text{O}_3$  to 102.7% for  $\text{P}_2\text{O}_5$ . Percentage recoveries for other metal oxides are 99.08 for  $\text{SiO}_2$ , 99.35 for  $\text{TiO}_2$ , 99.52 for  $\text{Al}_2\text{O}_3$ , 102.06 for  $\text{Fe}_2\text{O}_3$ , 101.11 for MnO, 100.74 for MgO, 100.37 for CaO and 99.73% for  $\text{Na}_2\text{O}$ .

### The geochemistry and mineralogy

The SEM-EDS results are presented using the backscattered electron (BE) images for each sample. Morphological measurement refers to grain size, shape and habit and aspect ratio, given as length x diameter measurement (L x D) were presented for every detected fibre and/or particle with serpentine and amphibole composition. The visible fibre size may not always correspond to actual size either because they are partially exposed or of submicron size. In case of fragment and bundle of fibres usually the visible dimensions of the longest and thinnest (smallest diameter) that might potentially be produced were measured.



Figure 4: Asbestos mine tailing closer to A, B, C, D and E study areas (from left to right).

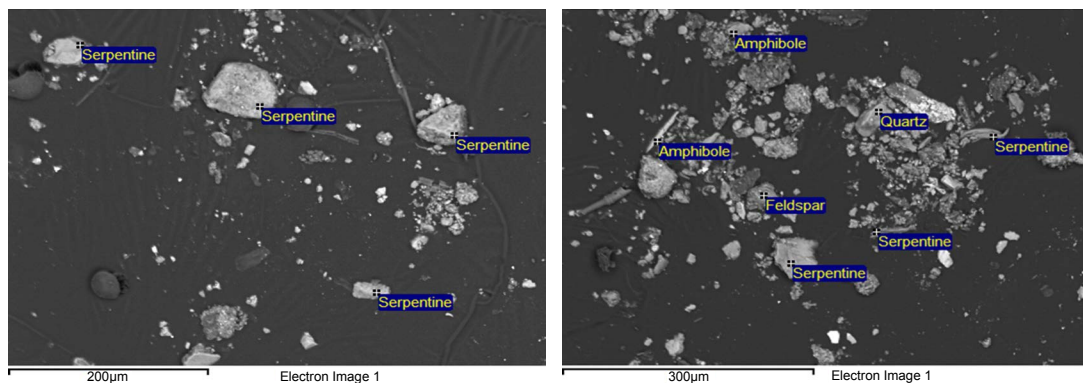


Figure 5 (a) and (b): SEM – EDS micrographs of trapped dust at Site A.

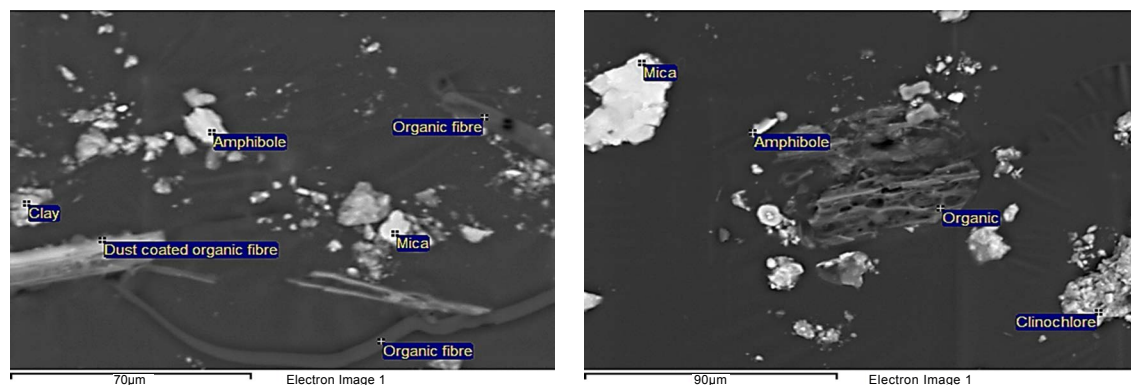


Figure 5 (c) and (d): SEM – EDS micrographs of trapped dust at Site B.

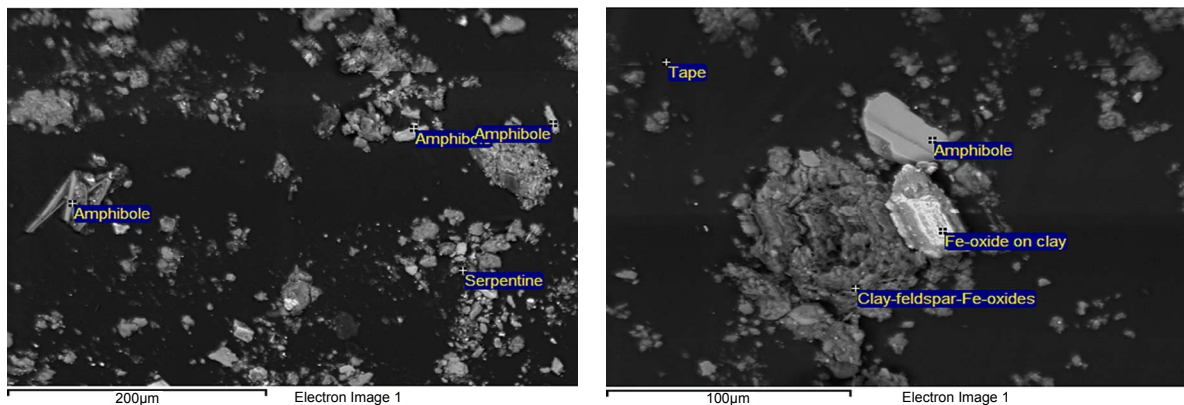


Figure 5 (e) and (f): SEM – EDS micrographs of trapped dust at Site C.

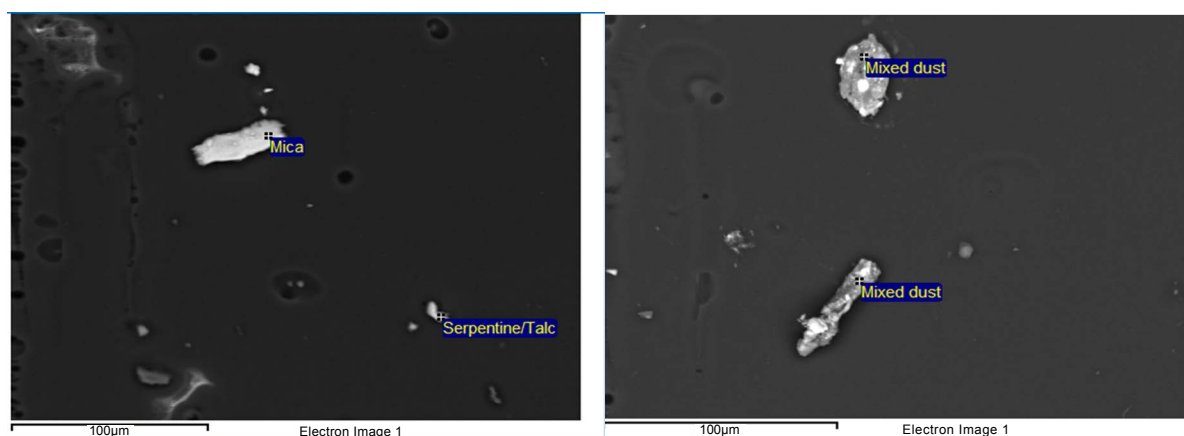


Figure 5 (g) and (h): SEM – EDS micrographs of trapped dust at Site D.

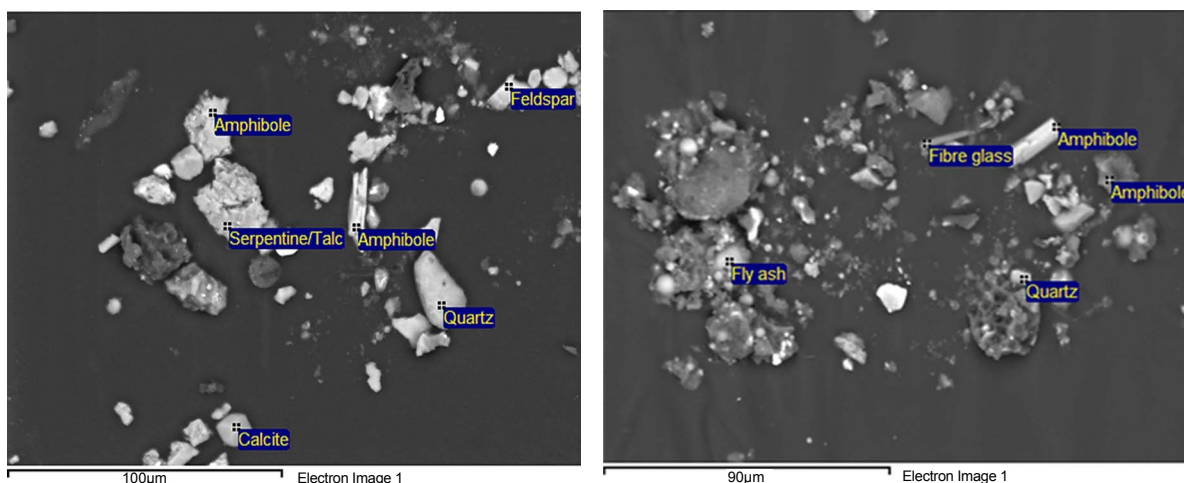


Figure 5 (i) and (j): SEM – EDS micrographs of trapped dust at Site E.

Figures (5a – 5j) are the SEM – EDS micrographs of dust trapped samples collected at different sampling sites. Both the serpentine and amphibole asbestos group of minerals were detected in all samples. The ratios between the serpentine and amphibole asbestos particles were determined by counting the number of each particle detected at each

sampling site. The serpentine to amphibole particle ratios are 7: 2 for site A; 0: 2 at site B; 1: 4 at site C; 1: 0 at site D and 1: 5 at site E. Site A is other detected minerals are characterized by aggregates of serpentine minerals detected with granular, semi triangular and semi- rectangular form having different aerodynamic diameters with the largest being

>100 µm. Other detected minerals are characterized by bundles of about 75 µm quartz and a semi spherical feldspar aggregate of particles.

Minerals of the serpentine group were not detected at Site B. However, a semi-rectangular bundle and a fibrous shape of amphibole minerals were detected with aerodynamic diameters ranging from about 10 to 25 µm. Large organic fibre (~150 µm), a sponge like organic material (~75 µm), dust coated organic fibre (~60 µm), organic fibre (~55 m), an aggregate of clinocllore minerals (~50 m), a bundle of mica (~45 µm) and an aggregate of clay (~25 µm) minerals were also detected at this site.

Site C is characterized a large bundle (~50 µm) and a fibrous (~55 µm) particle of amphibole minerals. A serpentine mineral particle of about 15 µm was also detected, together with minerals such as Fe-oxide (~30 µm) on a clay platform (~50 µm) and a large aggregate of clay-feldspar-Fe-oxides.

A serpentine / talc mixed particle of about µm aerodynamic diameter, a ~60µm rectangular like mica particle, a semi-rectangular mixed dust particles of ~80 µm and ~45 µm were detected at site D.

Trapped dust from site E is characterized by various types of minerals that have different shapes. A large aggregate mineral serpentine (~48 µm), a ~50 µm fibrous amphibole mineral, semi-triangular quartz particle (~51 µm), rectangular feldspar (~20 µm) and ~15 µm semi-spherical calcite particles. Fly ash particles which could be linked to industrial activities were also detected.

The results of the characterization of representative surface dust from two different sampling points per site by XRD are presented in Table 1. Both the serpentine (Mg<sub>3</sub>Si<sub>2</sub>O<sub>5</sub>(OH)<sub>4</sub>) and amphibole [Ca<sub>2</sub>(Fe, Mg)<sub>5</sub>Si<sub>8</sub>O<sub>22</sub>(OH)<sub>2</sub>] asbestos group of minerals are present in all the samples, but at different levels. Serpentine minerals were dominant with 68 and 56% m/m at sites A1 and A2, followed by 35% m/m at D2 and 31% m/m at E1. The intermediate asbestos serpentine levels ranged from 7 to 13% m/m at the remaining sites. Serpentine minerals were not detected in samples from sites C1 and E2. Low to trace levels of amphibole minerals were detected at all sites with the highest value of 15% m/m being detected at site C2.

Other common silicate minerals detected include quartz (SiO<sub>2</sub>), talc [Mg<sub>3</sub>Si<sub>3</sub>O<sub>10</sub>(OH)<sub>2</sub>], feldspar [(KAlSi<sub>3</sub>O<sub>8</sub>)-(NaAlSi<sub>3</sub>O<sub>8</sub>)-(CaAl<sub>2</sub>Si<sub>2</sub>O<sub>8</sub>)], Kaolinite (Al<sub>2</sub>Si<sub>2</sub>O<sub>5</sub>(OH)<sub>4</sub>), and smectite [(Na,Ca)0.33(Al, Mg)<sub>2</sub>(Si<sub>4</sub>O<sub>10</sub>)(OH)<sub>2</sub>.nH<sub>2</sub>O]. Trace levels of non-silicates minerals such as hematite (Fe<sub>2</sub>O<sub>3</sub>), chlorite (ClO<sup>2-</sup>), magnetite (Fe<sub>3</sub>O<sub>4</sub>), gibbsite [Al(OH)<sub>3</sub>],

dolomite [Ca-Mg (CO<sub>3</sub>)<sub>2</sub>] and ilmenite (FeTiO<sub>3</sub>) minerals were also detected. In a similar study on mine waste samples, [25] reported the detection of high levels of silicate minerals such serpentine, olivine [(Mg, Fe)<sub>2</sub>SiO<sub>4</sub>] and pyroxene [(XY(Si, Al)<sub>2</sub>O<sub>2</sub>] where X represents Ca, Na, Fe<sup>2+</sup> and Mg; Y represents smaller size ions such as Fe<sup>3+</sup>, Al, etc. Non-silicate chlorite, brucite [Mg(OH)<sub>2</sub>] and magnetite were also detected. Continental crust rocks were found to be composed mainly of quartz or feldspar [26].

The surface dust geochemistry results are presented in Table 2. The dominance of SiO<sub>2</sub> (28.78 to 84.71%) at all sites suggest that all the samples contain silicate minerals. Other dominant oxides compounds include MgO (14.94 to 41.20%) at sites A, B1 and C1; Fe<sub>2</sub>O<sub>3</sub> (10.65 to 38.45%) at sites A2, D2 and E and Al<sub>2</sub>O<sub>3</sub> (13.39%) at site B2. Minor to trace levels of metal oxides were also detected and have an intermediate rock composition, for example, TiO<sub>2</sub>, MnO, CaO, Na<sub>2</sub>O, K<sub>2</sub>O, P<sub>2</sub>O<sub>5</sub> and Cr<sub>2</sub>O<sub>3</sub>. A comparable study, [27] found oxygen (~46.6%) and silicon (~27.7%) to be the main constituents of silicates minerals on the earth's crust. Another similar bulk chemistry study of mine waste samples in the USA [25] reported main compounds as SiO<sub>2</sub> (34.4 to 40.3% m/m), MgO (35.2 to 38.8% m/m) and Fe<sub>2</sub>O<sub>3</sub> (6.91 to 12.3% m/m), as well as lesser levels of Al<sub>2</sub>O<sub>3</sub> (1.06 to 1.84% m/m).

The relatively high loss on ignition (LOI) results ranges from 7.21 to 17.69 m/m% at sites A, B, C, D2 and E are possibly due to H<sub>2</sub>O presence in asbestos compounds, hydrocalcite and dolomite carbonate minerals as presented in Table 2. This explanation is supported by the reported LOI levels of between 10.7 to 15.7 m/m % and accounted it to H<sub>2</sub>O presence in chrysotile and carbonates minerals such as the calcite, dolomite and hydrocalcite [25].

## Conclusion

The geochemical compounds detected confirm the dominance of silicate minerals on surface and trapped dust samples. Historically, the serpentine asbestos group mineral is known to have been mined and is associated with ultramafic igneous complexes in Mpumalanga province [13,14]. Therefore, the detection of the amphibole asbestos group of mineral within the study area was not surprising because of the abundance of silicates on the earth's crust. Also, different asbestos minerals could have been exposed during the mining of other commodities if they were present or existed as an accessory mineral in the province [12,15]. Particles linked to anthropogenic activities

Table 1: Common minerals detected from surface dust sampling sites (% m/m).

Two Sampling Points per Site	Hydrocalcite	Dolomite	Ilmenite	Magnetite/Magnessioferite	Hematite/Goethite	K-feldspar/Rutile	Plagioclase	Quartz	Mica	Kaolinite/Chlorite	Chlorite	Kaolinite	Amphibole	Serpentine	Talc	Gibbsite	Smectite
A1	3	4	-	-	-	-	-	trc	-	-	10	-	4	68	5	-	6
A2	-	-	-	9	2	-	-	27	-	-	5	-	-	56	-	-	-
B1	-	-	-	-	1	3	8	66	3	-	2	-	4	9	4	-	-
B2	-	-	-	-	2	-	-	72	-	10	-	-	2	7	3	-	4
C1	2	-	-	-	2	5	3	66	4	-	-	13	-	-	2	4	-
C2	2	-	-	-	5	14	27	-	-	-	-	20	15	13	-	4	-
D1	-	-	3	-	1	2	1	43	-	2	-	-	3	14	16	-	16
D2	-	-	-	-	9	-	2	39	-	3	-	-	2	35	10	-	-
E1	-	-	-	-	2	1	2	39	3	-	3	-	4	31	13	-	3
E2	-	-	-	-	5	-	8	66	3	13	-	-	3	-	2	-	-

**Table 2:** The geochemistry of bulk surface dust samples determined by XRF (% m/m).

Composition	A1	A2	B1	B2	C1	C2	D1	D2	E1	E2
SiO <sub>2</sub>	37.17	28.78	33.62	62.28	33.41	58.95	84.71	55.11	62.81	53.68
TiO <sub>2</sub>	0.21	0.40	0.05	0.59	0.02	0.60	0.16	0.30	0.84	0.36
Al <sub>2</sub> O <sub>3</sub>	4.87	5.32	1.96	13.39	1.39	14.14	5.23	8.41	8.58	7.58
Fe <sub>2</sub> O <sub>3(t)</sub>	4.48	38.45	9.61	8.01	6.00	9.61	2.47	11.12	12.66	10.65
MnO	0.247	0.279	0.079	0.159	0.114	0.181	0.030	0.183	0.252	0.298
MgO	38.02	14.94	40.94	2.20	41.20	1.54	2.86	16.63	2.09	11.12
CaO	0.84	0.35	0.01	1.39	0.37	0.44	0.01	0.07	0.76	0.63
Na <sub>2</sub> O	<0.01	<0.01	<0.01	1.08	<0.01	0.60	0.05	0.33	0.41	0.19
K <sub>2</sub> O	0.02	0.23	<0.01	0.74	<0.01	1.50	1.45	0.28	0.55	0.53
P <sub>2</sub> O <sub>5</sub>	0.046	0.144	0.020	0.176	0.014	0.212	0.023	0.021	0.255	0.087
Cr <sub>2</sub> O <sub>3</sub>	0.387	0.393	0.644	0.205	0.229	0.165	0.333	0.454	0.194	0.267
L.O.I.	14.40	10.39	12.32	9.72	17.69	11.88	1.64	7.21	10.74	14.75
<b>Total</b>	<b>100.46</b>	<b>99.64</b>	<b>99.00</b>	<b>99.94</b>	<b>100.17</b>	<b>99.83</b>	<b>98.96</b>	<b>100.13</b>	<b>100.14</b>	<b>100.14</b>

include the fly ash particles and glass fibres were also detected. Spherical shaped fly ash particles detected could be linked to coal burning power stations located in this province.

All the analytical results directly confirm the presence of both the serpentine and amphibole group of asbestos minerals in the samples. While the amounts detected are at trace levels, but the continued presence of the banned asbestos minerals around residential areas is of concern.

#### Acknowledgement

This research work was supported by the Council for Geoscience and The department of Mineral Resources. All analytical work was done at the Mineralogical Laboratory within the Council for Geoscience in Pretoria.

#### References

- Eberhard A (2011) The future of South African coal: Market, investment and policy challenges. Program on energy and sustainability development. Working paper.
- SAI (2016) IEEE Artificial Intelligence Conference – IntelliSys.
- Phillips JI, Rees D, Murray J, Davies JCA (2012) Mineralogy and malignant mesothelioma: The South African experience. Chapter 1.
- DEAT (Department of Environmental Affairs and Tourism) (2008) Emerging issues paper: Mine water pollution. Prepared by: Oelofse S. CSIR, Natural Resources and the Environment. March. ISBN NO: 978-0-9814178-5-1
- DMR (Department of Mineral Resources) (2009) The National strategy for the management of derelict and ownerless mines in South Africa.
- Van Eeden ES, Liefferink M, Durand JF (2009) Legal issues concerning mine closure and social responsibility on the West Rand. *The Journal for Transdisciplinary Research in Southern Africa*. 5: 51 -71.
- CGS (Council for Geoscience) (2015) Management of State contingent liabilities with respect to derelict and ownerless mines in South Africa. Proposal submitted to the Department of Mineral Resources.
- Braun L, Kisting S (2006) Asbestos-related diseases in South Africa. The social production of an invisible epidemic. *Public health then and now. American journal of Public Health*. 96: 1386 -1396.
- Davies TC (2015) Advances in mitigation and rehabilitation technology in major and abandoned mines in Sub-Saharan Africa. UNIVEN. IGCP/SIDA Project 594. Annual Workshop. Windhoek. Namibia. Czech Geological Survey. ISBN 978-80-7075-781-9. pp 17 -21.
- CMSA (Chamber of Mines of South Africa) (2015) Illegal mining in South Africa. Fact Sheet.
- Liebenberg Weyers D (2010) A multidisciplinary approach for the assessment of rehabilitation at asbestos mines in South Africa. Dissertation -Magister of Science in Environmental Science. Potchefstroom Campus of the North-west University.
- Makgae M (2014) The legacy of Asbestos mining in SA and its rehabilitation program. CAAWG 7. Presentation. Council for Geoscience.
- Deer WA, Howie RA, Zussman J (1992) Introduction to rock forming minerals. (2ndedn), Pearson Education Limited Publishers. Edinburg Gate. London.
- Ehlers DL, Vorster CJ (1998) Asbestos: The mineral resources of South Africa (6thedn), Council Geosciences, Hand book.
- Van Gosen BS (2010) The geology of natural asbestos deposits and its application to public health policy. U.S. Geological Survey. *Geology in China*. 37: 704 -711.
- USA-IM (USA Institute of Medicine) (2006) Selected health effects. Committee on Asbestos. Washington DC. National Academic Press.
- Gray A, Vawda Y, Jack C (2013) Health policy and legislation. *South African Health Review 2012/2013*. Durban: Health Systems Trust. In: Padarath A. English R, (eds). Published by Health System Trust.
- Kazan-Allen L (2016) Chronology of national asbestos bans. International ban asbestos secretariat. Revised 1 February.
- Mid-year Population Estimate (2015) Statistics, South Africa. 23 July. Retrieved on 6 July 2015.
- Census (2011) Census in brief: Pretoria Statistics South Africa. 2012. ISBN9780621413885
- Brandl G, Cloete M, Anhaeusser C R (2006) Archean green stone belt. In: Johnson MR., Anhaeusser, CR, Thomas RJ (eds), *The Geology of South Africa*. Geological Society of South Africa, Johannesburg. Council for Geosciences Pretoria pp 9-25.
- Nabhana S, Luber T, Scheffler F, Heubeck C (2016) Climatic and geochemical implications of Archean pedogenic gypsum in the Moodies Group (~3.2 Ga), Barberton Greenstone Belt, South Africa. *Precambrian Research*, 275, pp 119 -134.
- Valls D (2010) Soil and rock logging, classification and presentation manual. Caltrans edition. Department of Transportation. Division of Engineering Services Geotechnical Services. State of California.
- Atanasova M (2016) Determination of Asbestos in dust samples: Method for the analysis of filter dust samples and trapped surface dust samples by Scanning Electron Microscopy/Energy Dispersive Spectroscopy (SEM/EDS) and X-ray Diffraction (XRD). Mineralogical Laboratory at the Council for Geoscience. 04 April. TM-MIN001 Rev: 1
- Piatak NM, Deal II RR, Levitan DM, Hammarstrom JM (2009) Geochemistry of mine waste, mine drainage and stream sediments from the Vermont Asbestos Group Mine, Northern Vermont, USA. Paper presented at Securing the Future and 8th ICARD. June 23 -26, Skellefteå, Sweden.
- Shipman FT, Wilson JD, Todd AW (2003) An introduction to physical science. (10thedn). Houghton -Mifflin Publishers.
- Lutgens FK, Tarbuck EJ (2000) Essentials of geology. (2ndedn). WW Norton Publishers.